Effects of size and defects on the elasticity of silicon nanocantilevers

Hamed Sadeghian[1,2], **Chung-Kai Yang**[2], **Johannes F L Goosen**[1],
Andre Bossche[2], **Urs Staufer**[3], **Paddy J French**[2] **and Fred van Keulen**[1]

[1] Structural Optimization and Computational Mechanics (SOCM) Group, Department of Precision and Microsystems Engineering, Delft University of Technology, 2628 CD, Delft, The Netherlands
[2] Electronic Instrumentation Laboratory, Department of Microelectronics, Delft University of Technology, 2628 CD, Delft, The Netherlands
[3] Micro and Nano Engineering (MNE) Group, Department of Precision and Microsystems Engineering, Delft University of Technology, 2628 CD, Delft, The Netherlands

E-mail: H.SadeghianMarnani@tudelft.nl

Abstract

The size-dependent elastic behavior of silicon nanocantilevers and nanowires, specifically the effective Young's modulus, has been determined by experimental measurements and theoretical investigations. The size dependence becomes more significant as the devices scale down from micro- to nano-dimensions, which has mainly been attributed to surface effects. However, discrepancies between experimental measurements and computational investigations show that there could be other influences besides surface effects. In this paper, we try to determine to what extent the surface effects, such as surface stress, surface elasticity, surface contamination and native oxide layers, influence the effective Young's modulus of silicon nanocantilevers. For this purpose, silicon cantilevers were fabricated in the top device layer of silicon on insulator (SOI) wafers, which were thinned down to 14 nm. The effective Young's modulus was extracted with the electrostatic pull-in instability method, recently developed by the authors (H Sadeghian *et al* 2009 *Appl. Phys. Lett.* **94** 221903). In this work, the drop in the effective Young's modulus was measured to be significant at around 150 nm thick cantilevers. The comparison between theoretical models and experimental measurements demonstrates that, although the surface effects influence the effective Young's modulus of silicon to some extent, they alone are insufficient to explain why the effective Young's modulus decreases prematurely. It was observed that the fabrication-induced defects abruptly increased when the device layer was thinned to below 100 nm. These defects became visible as pinholes during HF-etching. It is speculated that they could be the origin of the reduced effective Young's modulus experimentally observed in ultra-thin silicon cantilevers.

(Some figures in this article are in colour only in the electronic version)

1. Introduction

Nanostructures, particularly those widely used in sensing and actuating applications, such as nanocantilevers, nanowires and nanotubes, have been attracting more and more interest due to their unique properties. They have shown unique electrical, photonic, thermal and mechanical properties as compared to their bulk counterparts. Consequently, great performances such as single-electron tunneling [1], sub-attonewton force sensing [2] and sub-femtometer displacement sensing [3], were achieved. For all these examples, use was made of the mechanical response of a nanostructure, which highly depends on the effective elasticity. In the past two decades, experimental measurements [4–8] and theoretical investigations, including *ab initio* and density functional theory (DFT) [9–11], molecular dynamics (MD) [12–15] and modifications to continuum theory [16–19], have been conducted toward characterizing the mechanical properties of nanostructures. The studies revealed a strong size dependence of the mechanical properties as the characteristic
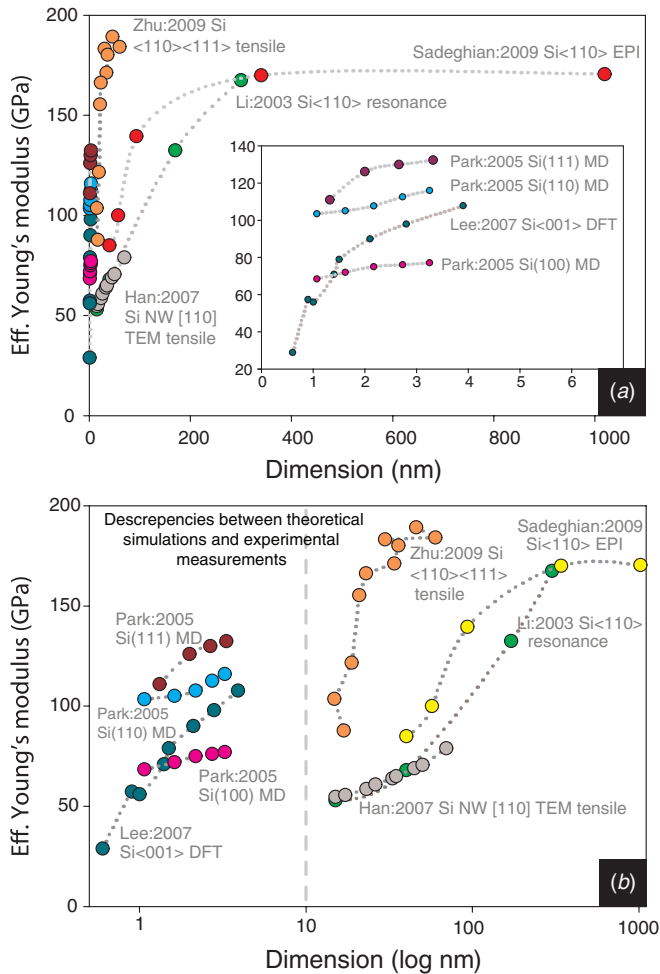
Figure 1. (*a*) Illustration of the size dependence of single-crystal silicon effective Young's modulus *E* obtained via simulation [11, 12] and experiments [4, 7, 20, 28]. The inset shows results for less than 10 nm. All simulation results are limited to thicknesses of less than 10 nm due to the computational complexity. (*b*) A logarithmic plot of (*a*) to further illustrate the differences between the simulation and the experiment results. Both show sharp drops near the down-scaling side; the discrepancies have been attributed to many effects but they are unconfirmed.

dimension-approached nanometer scales. However, a considerable discrepancy still remains between computational studies and experimental observations. As an example, the experimental results of single-crystal silicon [1 1 0] nanowires and nanocantilevers report the observed size dependence at about 150 nm [4, 20], while the computational investigations predict this to occur at a characteristic size of less than 10 nm [10, 12]. In order to visualize these discrepancies the results of the experimentally measured effective Young's modulus $\tilde{E}$ and those from simulations of silicon nanocantilevers and nanowires were collected from the literature and are shown in figure 1.

Figure 1 demonstrates that there is a rather large difference between the model predictions and experimental measurements. The simulated range of thicknesses which exhibits a decrease from the bulk value is much smaller than the range observed experimentally. The smallest experimentally tested silicon nanowires have an effective Young's modulus

of about one third of the bulk value, while the largest simulated nanowire has an effective Young's modulus that is much closer to the bulk value. The differences between the experimental results and the computational studies can potentially be ascribed to a number of causes. (1) It is extremely challenging to perform nanoscale experiments with desired resolutions and well-defined boundary conditions [21], especially when the size is below 50 nm. Experimental uncertainties, calibration and method (bending, resonance, tension) limitations influence the measurements. (2) Because it is computationally extremely expensive, it is impossible to model the atomistic systems as large as the ones tested experimentally, even in comparison to the smallest nanostructures ever tested. Although quasi-continuum approaches have been established as cost-reductive methods, they are lacking in certain important surface phenomena, such as surface reconstruction, defects emitted from free surfaces and surface stress induced phase transformations [22]. Due to the high surface-to-volume-ratio nature of nanostructures, the size dependence of the elastic behavior is generally attributed to surface effects, including surface elasticity [16, 19, 23], surface oxidation and surface contaminations [24, 25], while some have proposed that the nonlinear effect of the bulk elastic modulus is the main cause [26]. McDowell *et al* [27] studied the effects of geometry and surface structures on $\tilde{E}$ of metallic nanowires by atomistic simulation and concluded that, although these factors influence $\tilde{E}$ to some extent, they alone are insufficient to explain the experimentally observed trends. In addition, they have investigated the influence of the loading method on the measured $\tilde{E}$ and found that it affects only for dimensions below approximately 8 nm [14]. Another possible cause, yet to be investigated, is the effect of native oxide, which potentially would decrease $\tilde{E}$ through its distinct elastic response. Moreover, the nanocantilevers and nanowires are not defect-free and these can influence the experimentally measured data.

In this paper, we study the origin of the size dependence of $\tilde{E}$ in ultra-thin silicon cantilevers. The paper is organized as follows: the first part describes the fabrication process for ultra-thin silicon cantilevers, the second part is devoted to experimental measurements of $\tilde{E}$, the third part discusses possible effects and experimentally observed defects that may contribute to the decrease in $\tilde{E}$. Finally, conclusions and future work on the size dependence of $\tilde{E}$ are presented.

2. Fabrication of single-crystal silicon nanocantilevers

The cantilevers were fabricated from (1 0 0) smartcut® silicon-on-insulator wafers with a 1 μm buried oxide (BOX) and a 340 nm silicon device layer. For thinner cantilevers, the sample wafer was thermally oxidized and etched in HF to reduce the device layer thickness. For thicker cantilevers, single crystalline silicon was grown on the sample wafers by epitaxy. Cross-sections of the interface between the original surface and the grown layer were checked using a scanning electron microscope (SEM) and revealed a smooth continuation of the growth. Final thicknesses of all sample
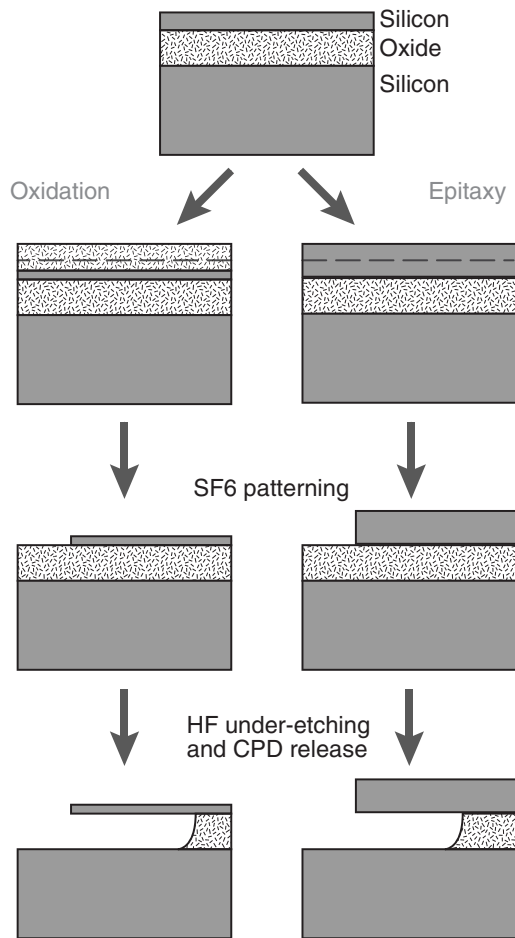
Figure 2. Schematic illustration of fabrication process, starting with SOI wafers with 340 nm thick device layer. The left column corresponds to cantilevers with thicknesses less than 340 nm. The right column corresponds to those thicker than 340 nm. The dashed lines are the original thicknesses of the SOI wafers.

wafers were determined by ellipsometry measurements with sub-nanometer accuracy. This was later used to indicate the influence of the errors in thickness and gap measurements on the error of the $\tilde{E}$ estimation. Cantilevers were patterned using standard photolithography followed by SF_6 chemistry plasma etching of the silicon device layer. The patterned structures were underetched in the HF solution to remove the BOX layer and released using the critical point drying. The final thicknesses were 1019, 340, 93, 57 and 40 nm. Figure 2 shows a schematic illustration of the fabrication procedure and figure 3 shows several SEM of the fabricated cantilevers. All the cantilevers have a width of 8 μm and length ranging between 8 and 200 μm. In order to ensure smoothness of the cantilevers' surfaces, the roughness of the surfaces was measured by AFM. The results confirm that the roughness of cantilevers' surfaces is in the sub-nm range. Figure 4 shows the AFM measurements of a 40 nm thick sample. The fabricated cantilevers were checked using an optical microscope and a SEM prior to pull-in measurements. The pre-bending of the cantilevers was checked by white light interferometry. Figure 5 shows a white light interferometric picture of a typical 340 nm thick cantilever (maximum tip deflection for the measured cantilevers was about 50 nm).

3. Experimental measurements

One of the challenges in studying the size-dependent behavior of nanostructures is to perform a meaningful experiment. A variety of experimental approaches have been developed to measure the mechanical properties of nanocantilevers. One popular approach is based on the analysis of the resonant behavior, where $\tilde{E}$ is extracted via the Euler–Bernoulli equation from fitted resonance frequencies [4, 29]. While resonance frequency approaches are widely used for characterizing mechanical properties, the experimental results include errors due to uncertainty of boundary conditions. Ding *et al* [30] investigated the effect of boundary conditions on the resonance frequency of nanowires; they showed that non-ideal boundary conditions lead to a lower resonance frequency, which leads to lower estimates of the effective Young's modulus. Moreover, native oxide, surface contaminations and other adsorbed layers cause changes in the mass and the stiffness of the system. Since it is almost impossible to decouple the stiffness from the mass changes solely by resonance response, consequently it is very difficult to estimate and analytically correct for the combined mass-stiffness effect. In many cases, the extra surface mass dominates the extra stiffness and decreases the resonance frequency [31], causing the interpreted $\tilde{E}$ to be lower than the actual value, making the measurement qualitative and rather unreliable in high surface-to-volume ratio structures.

Bending tests with an atomic force microscope (AFM) is another common approach to study the elastic behavior, as well as the strength of the nanocantilevers and nanowires. However, it also has considerable uncertainties in its measurement and interpretations. Errors result from difficulties in measuring the real deflection, preventing tip slippage [6], determining the contact area [5] and assessing the tip-cantilever indentation [5].

For the measurements of $\tilde{E}$, we opted for a recently developed technique using electrostatic pull-in instability (EPI) [7]. This technique has the advantages of easy setup, high accuracy, repeatability, as well as reproducibility. A typical setup of EPI is shown in figure 6, which involves a controllable voltage source and a standard probe station with a microscope. The details of the method can be found in [7]. For each thickness, the pull-in voltage and the geometry of the cantilevers with different lengths were measured. It needs to be noted that the undercut length ΔL created during the HF etching increases the effective lengths of the cantilevers. Previous work considering the undercut effects on cantilevers revealed that in order to compensate for the effect, ΔL has to be added to the original length of the cantilever [32, 33]. The pull-in data versus effective lengths ($\Delta L+L$) of the cantilevers were fitted to the electromechanical coupled equation [7], and $\tilde{E}$ for each thickness was determined. The maximum error of $\tilde{E}$ due to the errors of the cantilever's geometry measurements and the measured voltage was calculated to be 12% [7]. Figure 7 shows the experimental $\tilde{E}$ as a function of the thickness. As is clear from figure 7, $\tilde{E}$ is strongly thickness dependent and starts to decrease monotonically down from approximately 150 nm thick cantilevers. No length dependence of $\tilde{E}$ was observed in the experiments.
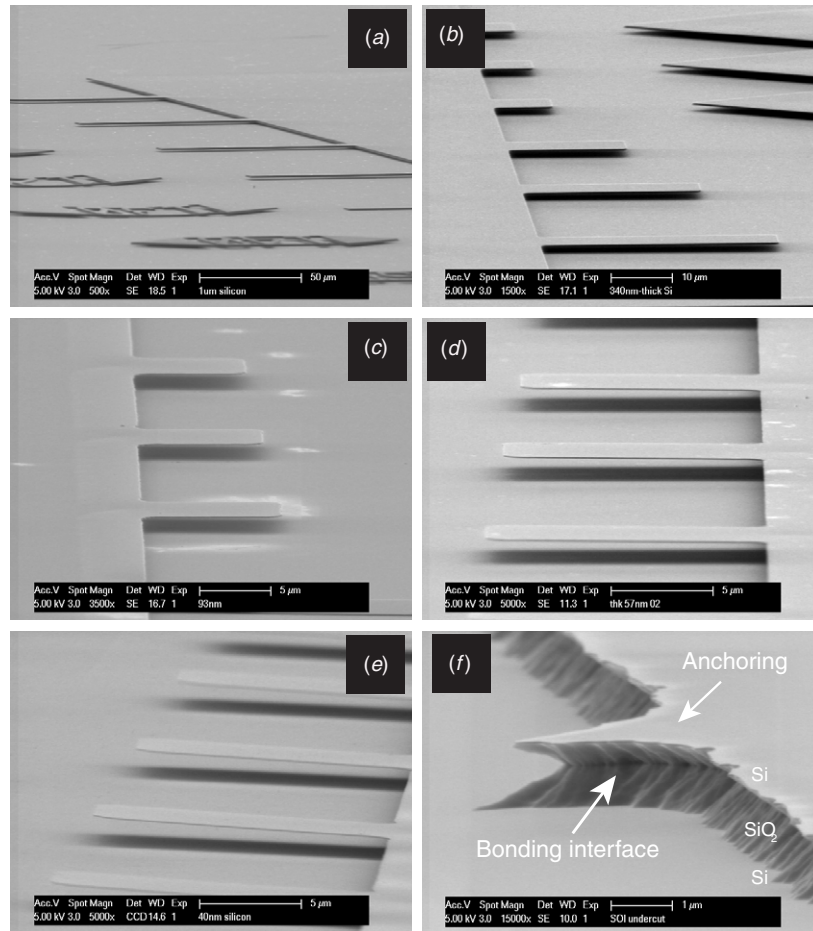
Figure 3. SEM of (*a*) 1019 nm, (*b*) 340 nm, (*c*) 93 nm, (*d*) 57 nm, (*e*) 40 nm thick cantilevers. (*f*) SEM of the buried oxide of a 40 nm thick device, the cantilever is forcefully removed, revealing the underneath oxide structures. The SOI wafer was bonded at the buried oxide layer, about 340 nm down from the top silicon. During HF etching, the chemical attacks the bonding interface faster and forms dents and holes in the oxide. The clamping points of the cantilevers are not flat, but have anchors as shown in the picture.
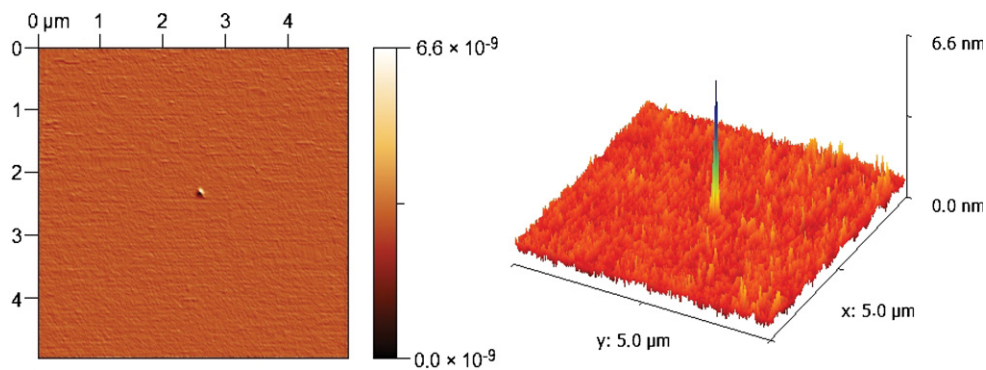
Figure 4. AFM measurement of the 40 nm silicon surface. The roughness measured has a root mean square of 0.155 nm.

4. Theoretical predictions: impact of surface elasticity and native oxide layers

Due to the small size and, thus, the large surface-to-volume ratio of nanocantilevers, the surface stress effects have been suggested as the explanation for the size effects [34]. As a result, the majority of research concerning the elastic response of nanostructures has focused on surface stress [35, 36] and

surface elasticity [16, 37, 38] effects. The origin of surface elasticity S comes from the difference between the energy associated with the atoms near the surface and those in the core of the bulk. The surface atoms, having lower coordination numbers and electron densities, tend to adopt equilibrium lattice spacings differently from the bulk ones. However, in order to retain the epitaxial relationship from bulk to surface, bulk atoms strain the atoms near the surface and create the
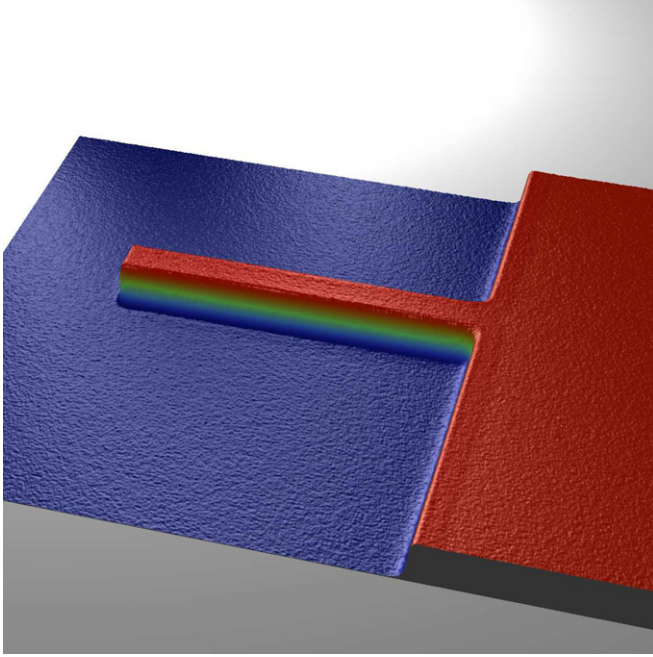
Figure 5. White light interferometric measurement of a 60 μm long silicon cantilever, showing that the cantilever is flat.
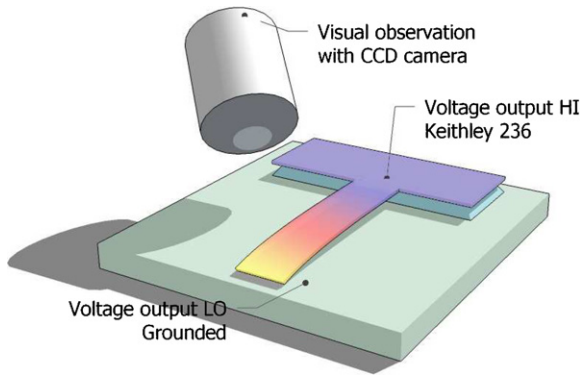
Figure 6. Schematic view of the electrostatic pull-in instability setup. The driving voltage on the cantilever is applied through a probe contact and the substrate is grounded.

so-called surface stress σ_s [39]. Due to σ_s, and the fact that semiconductor surface atoms like to reconstruct and can displace easily from their original places, the regions close to the surfaces have different elasticity compared to the bulk. Scaling down the device causes its surface-to-volume ratio to increase and therefore amplifies the influence of the surfaces.

A recently developed framework [19], which is an extension of previous models [16, 23, 38], was used to study the effect of surface elasticity on the size-dependent bending mode of $\tilde{E}$ as

$$E_s = E_b \left(1 + \frac{3 \Sigma S}{E_b t}\right) \quad (1)$$

where E_b is the bulk value of Young's modulus, known to be 169 GPa for [1 1 0] single-crystal silicon, ΣS is the sum of the surface elasticity at the top and the bottom surfaces, for which we assumed to be equal, and t is the thickness of the cantilever. The value of surface elasticity for silicon is about $-1 \, \mathrm{N\,m^{-1}}$
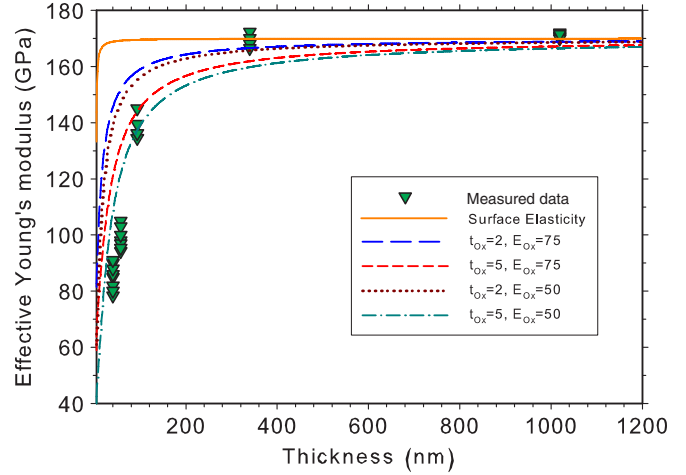
Figure 7. Measured $\tilde{E}$ of silicon nanocantilevers for different thicknesses. As the cantilevers become thinner, the difference between the measured data and the bulk value (the value for 1 μm thick cantilever) increases. The solid line shows the prediction of size dependence when considering surface elasticity, and the dashed and dotted lines show the prediction using equation (2), with additional native oxide layers taken into account.

[38, 40]. Considering only this surface elasticity effect, a size dependence can be calculated, and the results are plotted in figure 7 with a solid line.

The native oxide, on the other hand, influences $\tilde{E}$ both through its own distinct elastic response and unknown interactions between the oxide and the silicon at the interface. Here, we assumed that the effect of native oxide on the surface elasticity of silicon, or the interface elasticity of Si–SiO₂, is not significant compared to the distinct elastic response of the native oxide (the surface elasticity is about 0.1–1 N m⁻¹). By taking into account the surface elasticity of the original silicon and the elastic modulus of the native oxide layers E_{Ox}, $\tilde{E}$ can be estimated as

$$\tilde{E} = \frac{E_s t^3 + E_{Ox}\left(1 + \frac{3 \Sigma S}{E_b t}\right)(8(t_{Ox})^3 + 6t^2 t_{Ox} + 12t(t_{Ox})^2)}{(t + 2t_{Ox})^3} \quad (2)$$

where t_{Ox} is the thickness of the native oxide layer at the top and bottom of the cantilever. Since little is known about Young's modulus of the native oxide and its thickness, we calculated for different oxide thickness and Young's modulus values to see how changes of different parameter values influence $\tilde{E}$. The thicknesses of native oxide layers have been reported in the literature, ranging from 2 to 5 nm [6, 41]. Its Young's modulus also varies in the literature, reported between 50 and 75 GPa [42, 43]. The dashed and dotted lines in figure 7 show the resultant $\tilde{E}$ as a function of cantilever thicknesses considering the surface elasticity and different native oxide scenarios. From the figure it is observed that different oxide's properties partially explain the distinctive drops of $\tilde{E}$, but not fully. This shows that there might be more dominant effects influencing the trend. One possible effect that caught our attention is the fabrication-induced defects in the bulk crystal silicon.
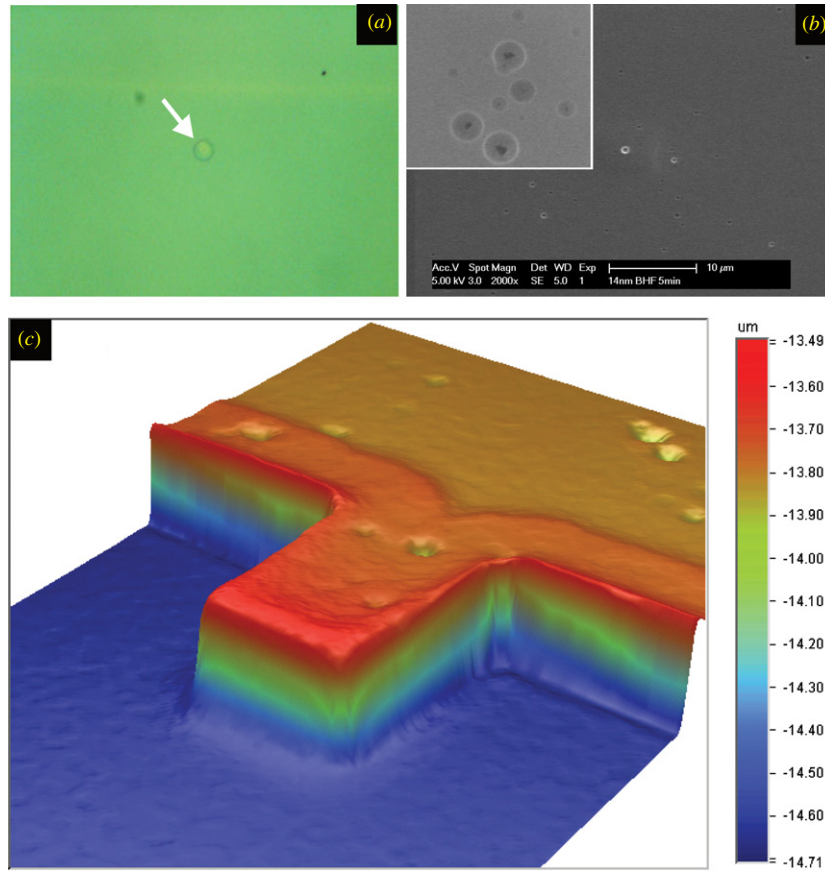
Figure 8. (*a*) Optical microscope image of a HF defect in a 14 nm-thick device layer of a SOI wafer. (*b*) SEM of HF defects in the 14 nm thick SOI wafer. The inset shows a close-up. The BOX layer below the HF defect is etched by the HF solution. (*c*) White light interferometric picture of a 40 nm thick cantilever with defects.

5. Fabrication-induced defects

As described in section 2, the SOI wafers were thinned down by alternating thermal oxidation and etching in the HF solution. It was observed that the density of fabrication-induced defects increased when reducing the thickness of the silicon device layer of SOI wafers.

The formation of the defects is known to occur during thermal oxidation processes, where the mismatching silicon and oxide lattices form stress in both layers [44]. When the top silicon layer becomes thin, defects and cracks form and can run through the whole layer thickness, like a pinhole, and exposing the underlying BOX. Without the top silicon protection, the exposed BOX can be easily removed when dipping the SOI wafer into HF etchant, leaving an undercut structure at the silicon crack site. Due to the simplicity, HF etching is often used to test the existence of these pinhole structures, and the resulting observed defects are called the HF defects. Figures 8(*a*) and (*b*) show, respectively, an optical and an electron microscopy of HF defects at a 14 nm thick silicon device layer. The HF defects are observed as circles with the defect at the center. The white light interferometric picture, shown in figure 8(*c*), shows the appearance of defects on the surface of the cantilever as well. It is suspected that the modification of structural properties of the device layer during

the oxidation thinning process, which appears in the form of HF defects, is one of the main reasons to the fast $\tilde{E}$ drop.

In order to approximate the effect of defects and pinholes on the $\tilde{E}$, an analytical solution, described in [45] is used as

$$E_d = E_0 \left(1 - \frac{A_d}{A_0} \right) \Big/ \left(1 + 2\frac{A_d}{A_0} \right). \quad (3)$$

It relates the relative area of defects and pinholes with respect to the total area of the structure (defect density) $\frac{A_d}{A_0}$, to the ratio of the effective Young's modulus with and without defect $\frac{E_d}{E_0}$. The result is shown in figure 9. It can be seen from the figure that increasing the defect density significantly changes $\tilde{E}$. This shows that the defects can be a main contribution to drops in $\tilde{E}$ of the experimentally tested nanocantilevers.

6. Discussions

As shown in figure 7, the experimental measurements as well as the theoretical results, considering surface effects and a native oxide layer, indicate a size dependence of $\tilde{E}$. However, the scale at which the size dependence starts, in experimental measurements, is different from that estimated theoretically. The experimental results showed that the size dependence starts at about 150 nm, whereas the results of the semi-continuum approach indicate size effects below 15 nm, i.e. very far from what experimental results
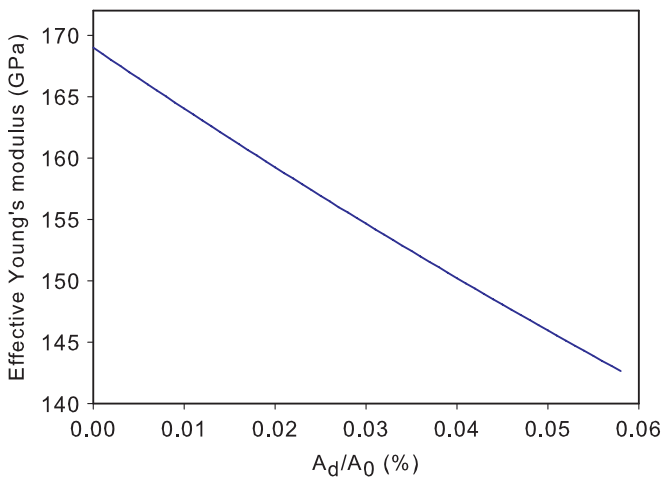
Figure 9. $\frac{E_d}{E_0}$ versus $\frac{A_d}{A_0}$. E_d and E_0 are the effective Young's modulus with defect and without defect, respectively.

showed. Taking the native oxide layer into consideration reduces the difference between experimental measurements and theoretical prediction, yet there is still a considerable difference. One can observe that the difference increases for thinner cantilevers. A number of models revealed that a structure with defects shows an additional decrease in $\tilde{E}$ [46]. It was observed here and in the previous work [44] that the density of fabrication-induced defects drastically increased when thinning down the SOI device layer.

7. Conclusions

In this paper, the size effects on the effective Young's modulus $\tilde{E}$ of single-crystal silicon nanocantilevers were experimentally as well as computationally investigated. The experimental results show a larger and earlier decrease in $\tilde{E}$ than the theoretical predictions, which are generally believed to be caused by surface effects. In this work, we directly compared the surface effects simulation with measured $\tilde{E}$ from the reliable EPI method and showed that other effects such as native oxides and HF defects should also be considered. As it turns out, the inclusion of these effects can explain the observed size-dependence trend. Therefore, the size dependence of $\tilde{E}$ is not dominated only by the surface effects, but also by other varieties of factors. Future work on the quantitatively determination of the defects, defect density as a function of thickness and their effects, will help to better explain the difference between experimental measurements and theoretical predictions on the size-dependent $\tilde{E}$ of silicon nanocantilevers. Additional research should look to more than surface effects, and search for other possible influences caused by the measuring method, material and environments.

References

[1] Steele G A, Huttel A K, Witkamp B, Poot M, Meerwaldt H B, Kouwenhoven L P and van der Zant H S J 2009 Strong coupling between single-electron tunneling and nanomechanical motion *Science* **325** 1103–7

[2] Mamin H J and Rugar D 2001 Sub-attonewton force detection at millikelvin temperatures *Appl. Phys. Lett.* **79** 3358–60

[3] Naik A, Buu O, LaHaye M D, Armour A D, Clerk A A, Blencowe M P and Schwab K C 2006 Cooling a nanomechanical resonator with quantum back-action *Nature* **443** 193–6

[4] Li X, Ono T, Wang Y and Esashi M 2003 Ultrathin single-crystalline-silicon cantilever resonators: Fabrication technology and significant specimen size effect on Young's modulus *Appl. Phys. Lett.* **83** 3081–3

[5] Agrawal R, Peng B, Gdoutos E E and Espinosa H D 2008 Elasticity size effects in zno nanowires; a combined experimental-computational approach *Nano Lett.* **8** 3668–74

[6] Gordon M J, Baron T, Dhalluin F, Gentile P and Ferret P 2009 Size effects in mechanical deformation and fracture of cantilevered silicon nanowires *Nano Lett.* **9** 525–9

[7] Sadeghian H, Yang C K, Goosen J F L, van der Drift E, Bossche A, French P J and van Keulen F 2009 Characterizing size-dependent effective elastic modulus of silicon nanocantilevers using electrostatic pull-in instability *Appl. Phys. Lett.* **94** 221903

[8] Zhu Y, Xu F, Qin Q, Fung W Y and Lu W 2009 Mechanical properties of vapor-liquid-solid synthesized silicon nanowires *Nano Lett.* **9** 3934–9

[9] Umeno Y, Kushima A, Kitamura T, Gumbsch P and Li J 2005 Ab initio study of the surface properties and ideal strength of (1 0 0) silicon thin films *Phys. Rev.* B **72** 165431

[10] Byeongchan L and Robert E R 2007 First-principles calculation of mechanical properties of Si⟨0 0 1⟩ nanowires and comparison to nanomechanical theory *Phys. Rev.* B **75** 195328

[11] Lee B and Rudd R E 2007 First-principles study of the Young's modulus of Si⟨0 0 1⟩ nanowires *Phys. Rev.* B **75** 041305

[12] Park S, Kim J, Park J, Lee J, Choi Y and Kwon O 2005 Molecular dynamics study on size-dependent elastic properties of silicon nanocantilevers *Thin Solid Films* **492** 285–89

[13] Woo S Hyun, Zhou L G, Hanchen H and Timothy S C 2005 Nanoplate elasticity under surface reconstruction *Appl. Phys. Lett.* **86** 151912

[14] McDowell M T, Leach A M and Gall K 2008 Bending and tensile deformation of metallic nanowires *Modelling Simul. Mater. Sci. Eng.* **16** 045003

[15] Kang K and Cai W 2007 Brittle and ductile fracture of semiconductor nanowiresmolecular dynamics simulations *Phil. Mag.* **87** 2169–89

[16] Miller R E and Shenoy V B 2000 Size-dependent elastic properties of nanosized structural elements *Nanotechnology* **11** 139–47

[17] Wang J, Huang Q-A and Yu H 2008 Size and temperature dependence of Young's modulus of a silicon nano-plate *J. Phys. D: Appl. Phys.* **41** 165406

[18] Wei G, Shouwen Y and Ganyun H 2006 Finite element characterization of the size-dependent mechanical behaviour in nanosystems *Nanotechnology* **17** 1118–22

[19] Sadeghian H, Goosen J F L, Bossche A and van Keulen F 2009 Surface stress-induced change in overall elastic behavior and self-bending of ultrathin cantilever plates *Appl. Phys. Lett.* **94** 231908

[20] Han X D, Zheng K, Zhang Y F, Zhang X N, Zhang Z and Wang Z L 2007 Low-temperature in situ large-strain plasticity of silicon nanowires *Adv. Mater.* **19** 2112–8

[21] Agrawal R and Espinosa H D 2009 Multiscale experiments: State of the art and remaining challenges *J. Eng. Mater. Technol.* **131** 041208

[22] Harold S P, Patrick A K and Gregory J W 2006 A surface cauchy-born model for nanoscale materials *Int. J. Numer. Methods Eng.* **68** 1072–95

[23] Dingreville R, Kulkarni A J, Zhou M and Qu J 2008 A semi-analytical method for quantifying the size-dependent elasticity of nanostructures *Modelling Simul. Mater. Sci. Eng.* **16** 025002

[24] Sadeghian H, Yang C K, Gavan K B, Goosen J F L, van der Drift E W J M, van der Zant H S J, French P J, Bossche A and van Keulen F 2009 Effects of surface stress on nanocantilevers *e-J. Surface Sci. Nanotechnol.* **7** 161–6

[25] Sadeghian H, Yang C K, Gavan K B, Goosen H, van der Drift E, van der Zant H, French P J, Bossche A and van Keulen F 2009 Surface contamination-induced resonance frequency shift of cantilevers *Proc. Int. Conf. on Nano/Micro Engineered and Molecular Systems* pp 400–3

[26] Liang H, Upmanyu M and Huang H 2005 Size-dependent elasticity of nanowires: nonlinear effects *Phys. Rev. B* **71** 241403

[27] McDowell M T, Leach A M and Gall K 2008 On the elastic modulus of metallic nanowires *Nano Lett.* **8** 3613–8

[28] Kizuka T, Takatani Y, Asaka K and Yoshizaki R 2005 Measurements of the atomistic mechanics of single crystalline silicon wires of nanometer width *Phys. Rev. B* **72** 035333

[29] McFarland A W, Poggi M A, Bottomley L A and Colton J S 2005 Characterization of microcantilevers solely by frequency response acquisition *J. Micromech. Microeng.* **15** 785

[30] Ding W, Calabri L, Chen X, Kohlhaas K M and Ruoff R S 2006 Mechanics of crystalline boron nanowires *Compos. Sci. Technol.* **66** 1112–24

[31] Craighead H 2007 Nanomechanical systems: measuring more than mass *Nature Nanotechnol.* **2** 18–9

[32] Gavan K B, van der Drift E W J M, Venstra W J, Zuiddam M R and van der Zant H S J 2009 Effect of undercut on the resonant behaviour of silicon nitride cantilevers *J. Micromech. Microeng.* **19** 035003

[33] Gavan K B, Westra H J R, Van der Drift E W J M, Venstra W J and van der Zant H S J 2009 Impact of fabrication technology on flexural resonances of silicon nitride cantilevers *Microelectron. Eng.* **86** 1216–8

[34] Schmid M, Hofer W, Varga P, Stoltze P, Jacobsen K W and No/rskov J K 1995 Surface stress, surface elasticity, and the size effect in surface segregation *Phys. Rev. B* **51** 10937–46

[35] Lachut M J and Sader J E 2007 Effect of surface stress on the stiffness of cantilever plates *Phys. Rev. Lett.* **99** 206102

[36] Hwang K S, Eom K, Lee J H, Chun D W, Cha B H, Yoon D S, Kim T S and Park J H 2006 Dominant surface stress driven by biomolecular interactions in the dynamical response of nanomechanical microcantilevers *Appl. Phys. Lett.* **89** 173905

[37] Wang G-F and Feng X-Q 2007 Effects of surface elasticity and residual surface tension on the natural frequency of microbeams *Appl. Phys. Lett.* **90** 231904

[38] Lu P, Lee H P, Lu C and O'She S J 2005 Surface stress effects on the resonance properties of cantilever sensors *Phys. Rev. B* **72** 085405

[39] Cammarata R C and Sieradzki K 1994 Surface and interface stresses *Annu. Rev. Mater. Sci.* **24** 215–34

[40] Sadeghian H, Goosen H, Bossche A, Thijsse B and van Keulen F 2009 Size-dependent elastic behavior of silicon nanofilms: molecular dynamics study *Proc. ASME 2009 Int. Mechanical Engineering Cong. and Exposition (IMECE2009)* pp 1–6

[41] Hsin C-L, Mai W, Gu Y, Gao Y, Huang C-T, Liu Y, Chen L-J and Wang Z-L 2008 Elastic properties and buckling of silicon nanowires *Adv. Mater.* **20** 3919–23

[42] Wang Z L, Dai Z R, Gao R and Gole J L 2002 Measuring the Young's modulus of solid nanowires by in situ tem *J. Electron Microsc.* **51** S79–85

[43] Yasumura K, Stowe T, Chow E, Pfafman T, Kenny T, Stipe B and Rugar D 2000 Quality factors in micron- and submicron-thick cantilevers *J. Microelectromech. Syst.* **9** 117–25

[44] Naumova O V, Vohmina E V, Gavrilova T A, Dudchenko N V, Nikolaev D V, Spesivtsev E V and Popov V P 2006 Properties of silicon nanolayers on insulator *Mater. Sci. Eng. B* **135** 238–41

[45] Shevlyakov Y A and Skoblin A A 1993 Relative stiffness of irregularly perforated plates *J. Math. Sci.* **65** 1389–95

[46] Broughton J Q, Meli C A, Vashishta P and Kalia R K 1997 Direct atomistic simulation of quartz crystal oscillators: Bulk properties and nanoscale devices *Phys. Rev. B* **56** 611–8